Vaccine 37 (2019) 7061–7069

Contents lists available at ScienceDirect

Vaccine

journal homepage: www.elsevier.com/locate/vaccine

Purification of flavivirus VLPs by a two-step chomatographic process

Túlio M. Lima [a,b], Matheus O. Souza [a,1], Leda R. Castilho [a,*]

[a] Federal University of Rio de Janeiro (UFRJ), COPPE, Cell Culture Engineering Laboratory, Av. Horácio Macedo, 2030 sl. G115, 21941-598, Cidade Universitária, Brazil
[b] Federal University of Rio de Janeiro (UFRJ), EQ, EPQB Graduate Program, Av. Horácio Macedo, 2030 sl. E206, 21941-598, Cidade Universitária, Brazil

ARTICLE INFO

Article history:
Available online 11 June 2019

Keywords:
Virus-like particles (VLPs)
Yellow fever virus
Zika virus
Downstream processing
Chromatographic purification

ABSTRACT

Flaviviruses are enveloped viruses with positive-sense, single-stranded RNA, which are most commonly transmitted by infected mosquitoes. Zika virus (ZIKV) and yellow fever virus (YFV) are flaviviruses that have caused significant outbreaks in the last few years. Since there is no approved vaccine against ZIKV, and since the existing YF attenuated vaccine presents disadvantages related to limited supply and to rare, but fatal adverse effects, there is an urgent need for new vaccines to control these diseases. Virus-like particles (VLPs) represent a recombinant platform to produce safe and immunogenic vaccines. Thus, based on our experience of expressing in recombinant mammalian cells VLPs of most flaviviruses circulating in the Americas, this work focused on the evaluation of chromatographic purification processes for zika and yellow-fever VLPs. The clarified cell culture supernatant was processed by a membrane-based anion-exchange chromatography and then a multimodal chromatographic step. With this process, it was possible to obtain the purified VLPs with a yield (including the clarification step) of 66.4% for zika and 68.1% for yellow fever. DNA clearance was in the range of 99.8–99.9%, providing VLP preparations that meet the WHO limit for this critical contaminant. Correct size and morphology of the purified VLPs were confirmed by dynamic light scattering (DLS) and transmission electron microscopy (TEM). The promising results obtained for both zika and yellow fever VLPs indicate that this process could be potentially applied also to VLPs of other flaviviruses.

1. Introduction

The *Flavivirus* genus, member of the *Flaviviridae* family, is composed of enveloped viruses with positive-sense, single-stranded RNA, which are most commonly arthropod-borne viruses usually transmitted by infected mosquitoes. Dengue virus (DENV) is an example of a flavivirus that has challenged the public health worldwide for decades. Besides DENV, zika virus (ZIKV) and yellow fever virus (YFV) have also become noteworthy threats due to the significant outbreaks that took place in the last few years [1–4].

ZIKV was discovered in 1947 in Uganda, and in 2007 and 2013 it caused isolated outbreaks in Pacific Islands [5]. In 2015 the virus was detected for the first time in Brazil and since then quickly spread to over 80 countries. By the beginning of 2018, there was an accumulated number of 223,477 confirmed cases just in the Americas with 5885 imported cases in the United States [6]. Most zika patients are asymptomatic, but in a small proportion of adults ZIKV infection may lead to Guillain-Barré syndrome, and in a considerable proportion of pregnant women ZIKV infection may cause serious congenital malformations in the fetuses, particularly in the central nervous system [7]. Furthermore, ZIKV can be transmitted by the sexual route and can persist for extended periods in body fluids (including sperm) [8,9]. Thus there is a great need for the development of a vaccine to prevent the spread of the virus to non-endemic countries, and to prevent periodic outbreaks in regions where the virus is already circulating.

Yellow fever virus is a highly lethal virus, that causes death in about 10% of non-vaccinated individuals [10,11]. In past centuries, before the introduction of the current live-attenuated vaccine, 6–10% of the population of cities like Philadelphia (USA) and Barcelona (Spain) died in YF outbreaks [12,13]. The current vaccine is very safe and provides life-long protection from a single dose, but it can cause fatal adverse effects in a small proportion of vaccinees, and the egg-based production is limited in capacity. This latter fact led to severe vaccine shortages during an outbreak in Africa in 2016 and in Brazil in 2017–2018 [14,15]. During the African outbreak in 2016, the WHO introduced the use of a fractional dose (1/5) as an emergency measure to control outbreaks [16–18], but even with the use of fractional doses, shortage

* Corresponding author.
E-mail address: leda@peq.coppe.ufrj.br (L.R. Castilho).
[1] Current address: The University of Kansas, Department of Pharmaceutical Chemistry, Immune Engineering Laboratory, 2095 Constant Ave., Lawrence, KS 66047, USA.

https://doi.org/10.1016/j.vaccine.2019.05.066
0264-410X/

of the current vaccine would be an issue if YFV spreads and especially if it gets to be locally transmitted in Asia, where the mosquito vector is widespread [19].

Virus-like particles (VLPs) arise in this context as a feasible alternative to traditional vaccines. These particles are constituted by recombinant structural proteins of the virus, lacking the viral genome and mimicking the architecture of native viruses, representing a safe and potentially cost-effective platform for the development of vaccines for flaviviruses [20–22]. The purification of VLPs and virions is usually performed by polyethylene glycol precipitation, diafiltration, density gradient ultracentrifugation, ultracentrifugation or continuous flow ultracentrifugation. Although these techniques are vastly used, they present critical limitations, such as: host cell-derived contaminants in the case of precipitation, disruption of particles that affects immunogenicity in sucrose gradient centrifugation, expensive equipment required for continuous flow ultracentrifugation, and safety hazards concerning ultracentrifugation of viruses. Those disadvantages can be overcome through the use of chromatographic processes that are easily scalable, comparatively cost-effective, and that can lead to high purity, potency and consistency [23,24].

In this work, a two-step chromatographic process was studied for the purification of zika and yellow fever VLPs from HEK293-derived cell culture supernatant, building on a process proposed by Pato et al. for the purification of whole yellow fever virus from Vero cell culture [25,26]. The initial clarification of the cell culture suspension was performed by centrifugation and/or filtration, followed by anion-exchange chromatography and then a multimodal chromatographic step. The anion exchanger used was a Q membrane adsorber, due to its easy scalability, simplicity to handle, absence of diffusional limitations, and good performance at high flow rates for the capture of large molecules and particles such as VLPs [23,25–28]. This capture step allowed a high degree of concentration and an efficient DNA removal. To enhance clearance of host cell proteins (HCP), a CaptoCore 700 multimodal column was used in flow-through (FT) mode, allowing contaminants to be adsorbed while VLPs were excluded by size [26,29]. Samples from all steps of the process were characterized by immunoassays, total protein determination, SDS-PAGE and Western blot. Selected samples were further characterized by transmission electron microscopy (TEM) and dynamic light scattering (DLS).

2. Materials and methods

2.1. Cell culture and VLP production

Stable HEK293SF-3F6 (NRC, Canada) cells constitutively expressing VLPs made of the pre-membrane and envelope proteins of either ZIKV (strain BeH819966, GenBank #KU365779.1) or YFV (strain BeH622493, GenBank #JF912188) were utilized for VLP production [30]. Cells were grown in batch mode using Erlenmeyer flasks with 250 mL working volume at 37 °C, 5% CO_2 and 180 rpm, using the animal-component free, chemically defined medium HEK-TF (Xell AG, Germany) supplemented with L-glutamine. After each batch, the cell suspension was centrifuged at 1000 g for 10 min and cells were used for a repeated batch. The supernatants collected from different batches were pooled and kept in sterile aliquots at 4 °C until purification experiments were carried out. VLP concentration in the supernatant pools were 15.8 and 14.7 μg/mL for zika and YF VLPs, respectively. These concentrations decreased to 13.3 and 11.7 μg/mL, respectively, after clarification of the supernatants. The breakthrough curve to determine the dynamic binding capacity (Section 3.1, Fig. 1C) was the only experiment performed with a different supernatant pool.

2.2. Clarification

Prior to purification experiments, the supernatant aliquot was again centrifuged at 2000*g* for 10 min and filtered with a nitrocellulose membrane with nominal pore size of 0.45 μm (Millipore, USA).

2.3. Chromatographic purification

The downstream process was based on the procedure developed for the purification of whole YF virus by Pato et al. [25,26] and adapted for the purification of yellow fever and zika VLPs by altering in the first step the elution conditions and replacing the Tris buffer by phosphate buffered saline (PBS). The purification was performed in two chromatographic steps, using the anion-exchange chromatography membrane Sartobind® Q nano 3 mL (Sartorius, Germany) operating in bind-and-elute mode, followed by a multimodal chromatography step using a 1-mL HiTrap CaptoCore 700 column (GE Healthcare, Sweden) operating in

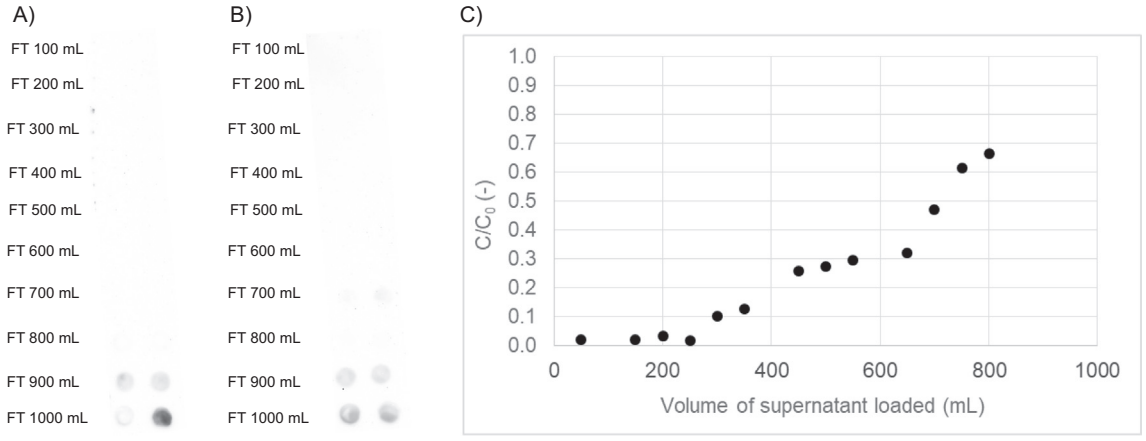

Fig. 1. Investigation of the binding capacity of the 3-mL Sartobind Q membrane adsorber. Immunoblot of the flow-through (FT) fractions collected at every 100 mL during anion-exchange membrane loading with 1 L clarified supernatant containing (A) 13.3 μg/mL zika VLPs and (B) 11.7 μg/mL yellow fever VLPs. (C) Breakthrough curve to determine the dynamic binding capacity: a volume of 800 mL of clarified HEK293 cell culture supernatant containing zika VLPs (22 μg/mL) was loaded onto the membrane adsorber, and the concentration (C) of VLPs leaking in the flow-through fractions was measured by ELISA and normalized to the feed (C_0) concentration.

flow-through mode. Both chromatographic steps were performed using an ÄKTA Purifier protein purification system controlled by the software Unicorn 5.20 (GE Healthcare, Sweden). For all chromatographic experiments flow rate was 10 mL/min, and fractions were collected in 10 mL aliquots unless stated otherwise.

Two buffers were used for both steps of the chromatography process. Although the original process proposed by Pato et al. [25,26] used Tris-buffer, we verified that PBS could be used instead. Buffer A was PBS (0.0027 M KCl, 0.01 M Na_2HPO_4, 0.0018 M KH_2PO_4, pH 8.0) and buffer B was 1 M NaCl in PBS (pH 8.0). These buffers were used in different proportions in all stages (equilibration, washing, elution) of the capture step, as well as for CaptoCore equilibration.

At first, in order to evaluate the capacity of the Q membrane to adsorb VLPs, 1 L of clarified supernatant (of either zika VLPs or YF VLPs) was loaded onto the membrane and the flow-through samples were analyzed by immunoblot. In order to gain a further insight into the dynamic binding capacity for VLPs a large volume of zika VLP feed (800 mL) was loaded onto the Q membrane, and the flow-through fractions were analyzed by ELISA. Purification runs were then carried out maximizing the volume of supernatant fed according to the binding capacity observed in these experiments.

The Q membrane was equilibrated with 9% of buffer B in order to match the conductivity of the cell culture supernatant, followed by feeding of the clarified supernatant. In order to determine the best conditions for washing and elution, the membrane adsorber was fed with supernatant (of either zika VLPs or YF VLPs) and then successive steps with increasing NaCl concentration (9% to 48% of buffer B) were performed. The duration of each step was chosen to ensure that the base line was recovered after each peak. The eluate fractions were analyzed by immunoblot. The final conditions chosen for the Q membrane step comprised two washing steps at 9% and then 12% of buffer B, followed by a elution step at 35% of buffer B. Finally, the membrane was regenerated by a wash with 100% buffer B, followed by a wash with 1 M NaOH.

The second chromatography step was performed with a multimodal resin. After equilibration with 35% of buffer B (to match the elution conditions of the previous step), the Q eluate was injected into the column and the purified VLPs were recovered in the flow-through fraction, since they are excluded by the shell of the CaptoCore 700 resin. The resin was then regenerated by a wash with 30% isopropanol in 1 M NaOH.

VLP, DNA and total protein concentration were analyzed in the samples to determine the performance of the chromatography runs, and the purified VLPs were further evaluated by transmission electron microscopy and dynamic light scattering (DLS) to evaluate the size and morphology of the VLPs.

2.4. VLP quantification

VLP concentration was measured using a quantitative sandwich ELISA, using as capture antibody the 4G2 monoclonal antibody produced and purified by LATAM (Biomanguinhos/FIOCRUZ, Brazil) and as secondary antibody also 4G2 monoclonal antibody, but biotinylated using the EZ-Link™ Sulfo-NHS-LC-Biotinylation Kit (ThermoFisher Scientific, USA). Detection was carried out by incubating the plates with TMB Single Solution (Invitrogen, USA), stopping with 1 M HCl and reading the absorbance at 450 nm. Washing between ELISA steps was done using PBS buffer with 0.05% (v/v) Tween 20. The 4G2 monoclonal antibody recognizes the conserved fusion-loop region of the envelope protein of flaviviruses, and it was used in both steps of the assay in order to minimize detection of monomeric E protein. The standard curve for zika VLPs was made using a commercial recombinant zika VLP (Native Antigen Company, UK). For yellow fever a sample of VLPs produced and purified in house, quantified by total protein analysis, was used as standard.

2.5. Total protein assay

The total protein (TP) concentration in samples from each step was evaluated using the Bio-Rad Protein Assay (Bio-Rad, USA) based on the Bradford dye-binding method, according to the manufacturer's instructions. Bovine serum albumin was used as standard.

2.6. DNA assay

The DNA concentration of each sample was measured using the PicoGreen dsDNA Assay kit (Invitrogen, USA), according to manufacturer's instructions.

2.7. Immunoblots

Two variants of immunoblots (Western blot and spot blot) were performed in order to confirm the presence of the VLPs. Western blots were carried out after a non-reducing SDS-PAGE was performed, applying to each lane samples from different steps of the process. Samples were normalized for the VLP mass measured by ELISA. Proteins were then transferred to a nitrocellulose membrane and marked with 4G2 antibody followed by an anti-mouse HRP-conjugated monoclonal IgG (Invitrogen, USA). ECL Prime (GE Healthcare, Sweden) was added for chemiluminescent imaging.

To investigate the presence of glycans in the yellow fever VLPs produced in HEK293 cells, VLP samples were treated with 8.3 IU/mL PNGase F (New England Biolabs, USA) and 2% (v/v) SDS for 3 h at 37 °C and then analyzed by Western blot.

For spot blots, 3 μL of each sample was pipetted onto a nitrocellulose membrane, and after drying the membrane, it was incubated with 4G2 and HRP-conjugated antibodies, washed and stained with ECL Prime as described above for Western blotting.

2.8. Transmission electron microscopy (TEM)

Microscopy images were obtained by Prof. Lucio Caldas (CENABIO/UFRJ, Brazil) by negative staining with either uranyl acetate or aurothioglucose. The microscope used was a FEI Tecnai T20 at 200 kV with a MegaView G2 1k1k-vi camera.

2.9. Dynamic light scattering (DLS)

A NanoBrook 90 Plus Particle Size Analyzer and a ZetaPals Zeta Potential Analyzer (both Brookhaven Instruments Corporation, USA) were used to determine the size distribution of the purified VLPs by detecting the intensity of the light scattered at the angles of 15°, 90° and 173°, or only at 15°, respectively.

3. Results and discussion

Pato et al. [25,26] proposed a 2-step downstream process for whole yellow fever virus propagated in Vero cell culture. We made *in silico* predictions of the pI of the E protein of YFV and ZIKV, and verified the similarity of both. Therefore we postulated that the process proposed in [25,26], which is based on an ion-exchange step followed by a second step where size of the viral particles is decisive, could be adapted for the purification of VLPs of a range of flaviviruses. This work shows our studies to adapt the process to the purification of yellow fever and zika VLPs produced in recombinant HEK 293 cells.

Since the buffer (50 mM Tris buffer, pH 8.5) used in [25,26] presents some disadvantages, such as higher costs and a high degree of pH sensitivity to temperature [31], we decided to replace it by phosphate buffer saline (PBS), adopting pH 8.0 as a compromise between Pato's results [25] and the buffering strength of PBS.

The following sections show the studies that we carried out to investigate the binding capacity for zika and YF VLPs in the capture step (Q membrane adsorber), the best elution conditions in the Q membrane adsorber, and the performance of the complete 2-step purification process. The promising results obtained demonstrate that the buffer modification was successful, lowering buffer costs and supplying VLPs in PBS, which is more compatible to the applications of the purified VLPs.

3.1. Evaluation of dynamic binding capacity and optimal elution conditions

For the capture of the VLPs from clarified HEK293 cell culture supernatant, a Q strong anion exchange membrane adsorber was used as first chromatography step. At first, it was important to determine the dynamic binding capacity of the VLPs to the Q membrane, in order to avoid loss of VLPs in the flow-through and to maximize recovery.

One liter of clarified cell culture supernatant containing either zika or YF VLPs was applied to a 3-mL nano Q adsorber, and samples of the flow-through were collected and analyzed by immunoblot for the presence of VLPs (Fig. 1A and B). For zika VLPs, a further experiment was carried out loading 800 mL of supernatant onto the Q membrane and quantifying the VLP concentration in the flow-through samples by ELISA. Fig. 1C shows the breakthrough curve for zika VLPs. It can be observed that approximately 6.6 mg of VLPs (300 mL of clarified supernatant containing 22 μg/mL of VLPs) bound to the 3-mL membrane adsorber before breakthrough of 10% of VLP present in the feed occurred. Based on this experiment, we can estimate that the dynamic binding capacity at 10% breakthrough (DBC10) is of approximately 2.2 mg VLP per mL of membrane bed at the flow rate used (10 mL/min). Since this membrane adsorber is available up to membrane bed volumes of 5000 mL, this means that, considering the DBC10, a large-scale process could potentially process a VLP mass in the order of 11 g per cycle, provided the dynamic binding capacity remains in the same range for the larger units.

Because the purification factor of an ion-exchange chromatography step relies also on the elution conditions, based on the slight variations in pI and in the composition of the HEK293 cell culture supernatant as compared to the Vero supernatant containing whole YF virus used in [25,26], we decided to study what the optimal conductivity (given by the concentration of NaCl) would be for elution of each VLP. With this aim, as shown in Fig. 2A for zika VLPs and in Fig. 2C for YF VLPs, 1 L of supernatant was loaded onto the Q membrane adsorber and elution was carried out by successively increasing NaCl in steps of 60 mM (6% of buffer B). The spot blots

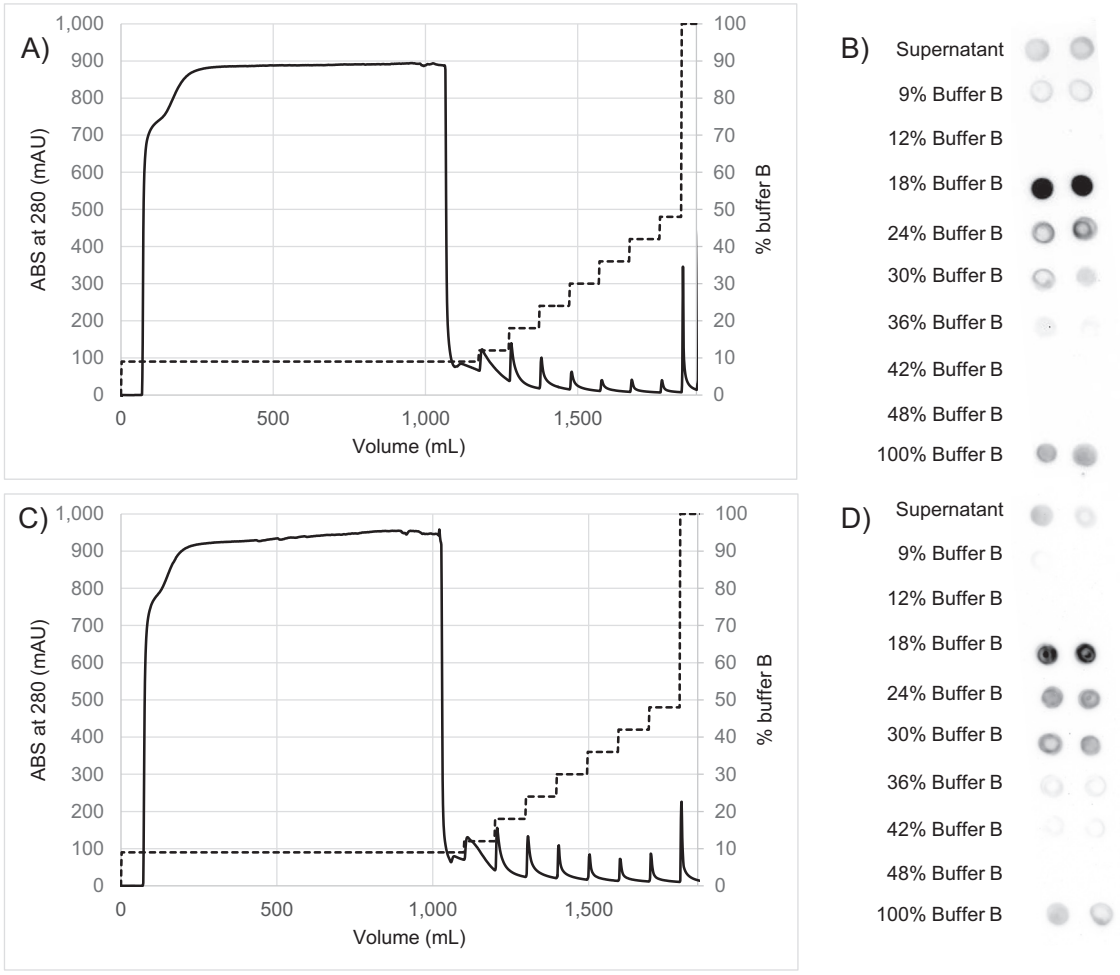

Fig. 2. Investigation of elution conditions for the anion-exchange capture step. Chromatograms showing elution steps carried out at increasing NaCl concentrations (% of buffer B) for zika (A) and yellow fever (C) VLPs, and the corresponding immunoblots showing samples eluted at the successive steps for zika (B) and yellow fever (D) VLPs. In A and C, solid lines represent the absorbance at 280 nm and dashed lines represent the concentration of buffer B.

in Fig. 2B (zika VLPs) and 2D (YF VLPs) show that VLPs were mainly detected in the peaks corresponding to 180–300 mM NaCl (18–30% buffer B). For both VLPs, a very light signal could be observed for 36% B (360 mM NaCl). Since this anion-exchange technique is used as capture step, we decided to prioritize yield over purification factor, and established as standard protocol for both VLPs the use of: (i) 9% B for equilibration and first wash (since 90 mM NaCl in PBS resulted in approximately the same conductivity as the supernatant); (ii) 12% B for a second wash, in order to remove impurities binding weakly to the Q adsorber; (iii) 35% B for elution, in order to maximize recovery of VLPs; and (iv) 100% B, in order to remove strongly bound impurities prior to the regeneration step (NaOH wash) of the adsorber. Thus, in the process as defined herein, conductivity for the second wash was 13.6 mS/cm (120 mM NaCl in PBS) and 33.7 mS/cm for elution (350 mM NaCl in PBS). In the work by Pato et al. [25], after evaluating the performance of the Q step, the authors decided to use 150 mM NaCl in 50 mM Tris buffer (15.6 mS/cm conductivity) for washing and 300 mM NaCl in 50 mM Tris buffer (28.4 mS/cm) for elution.

3.2. Two-step purification

After establishing in 3.1 the conditions for the capture step, the complete 2-step process was carried out for both zika and YF VLPs. The second chromatography step is based on the multimodal resin CaptoCore 700, where the VLPs are excluded by size and the impurities bind to the resin core. In an attempt to keep the process as simple as possible, and following the methodology used in [26], equilibration and feed of the multimodal step were carried out in the same buffer as VLPs had been eluted from the Q membrane, which opens up prospects for integrating both chromatography steps in a straight-through strategy [32].

Typical chromatograms for the Q capture and the CaptoCore step are shown in Fig. 3 for zika (3A, 3C) and YF (3B, 3D) VLPs. The eluted fraction collected from the anion-exchange membrane was injected onto CaptoCore 700 resin, and all the volume of the CaptoCore flow-through fraction was collected as purified material. The presence of VLPs in the peak eluted from the Q membrane adsorber, collected in 3 mL aliquots, was confirmed by immunoblot, while little to no signal was observed in all other fractions as shown in Fig. 4.

The clarified supernatant and all fractions collected from each chromatographic step were analyzed by ELISA in terms of VLP concentration, total protein (TP) and DNA concentration. These data allowed evaluating the performance of the process in terms of: yield, based on the VLP mass recovered; purification factor, comparing the ratio of VLP mass to total protein mass in each step; total protein and DNA removal, considering the TP or DNA mass removed in each step (Table 1).

Due to the large size of the VLPs and the pore size distribution of microfiltration membranes around the nominal cut-off, the clarification step caused a loss of 16–20% of VLPs. The anion-exchange step resulted in 86.7% and 95.5% VLP recovery for zika and YF VLPs respectively, which is higher or comparable to values found by other authors for whole virus or VLPs, with similar DNA clearance [25,26,33]. In the second step, using the CaptoCore column, a recovery of approximately 90% was found for both VLPs, which is higher than the reported for whole yellow fever virus [26], enterovirus VLPs [34] and adenovirus type 5 VLPs [35]. Thus, with this process, it was possible to obtain the purified VLPs with an overall yield (considering the clarification and the two chromatographic steps) of 66.4% for zika VLPs and 68.1% for yellow fever VLPs. This process also enabled a total protein removal of 95.5% and 91.4%, and a DNA removal of 99.8% and 99.9% for zika and YF VLPs, respectively. The final concentration of total protein in the purified

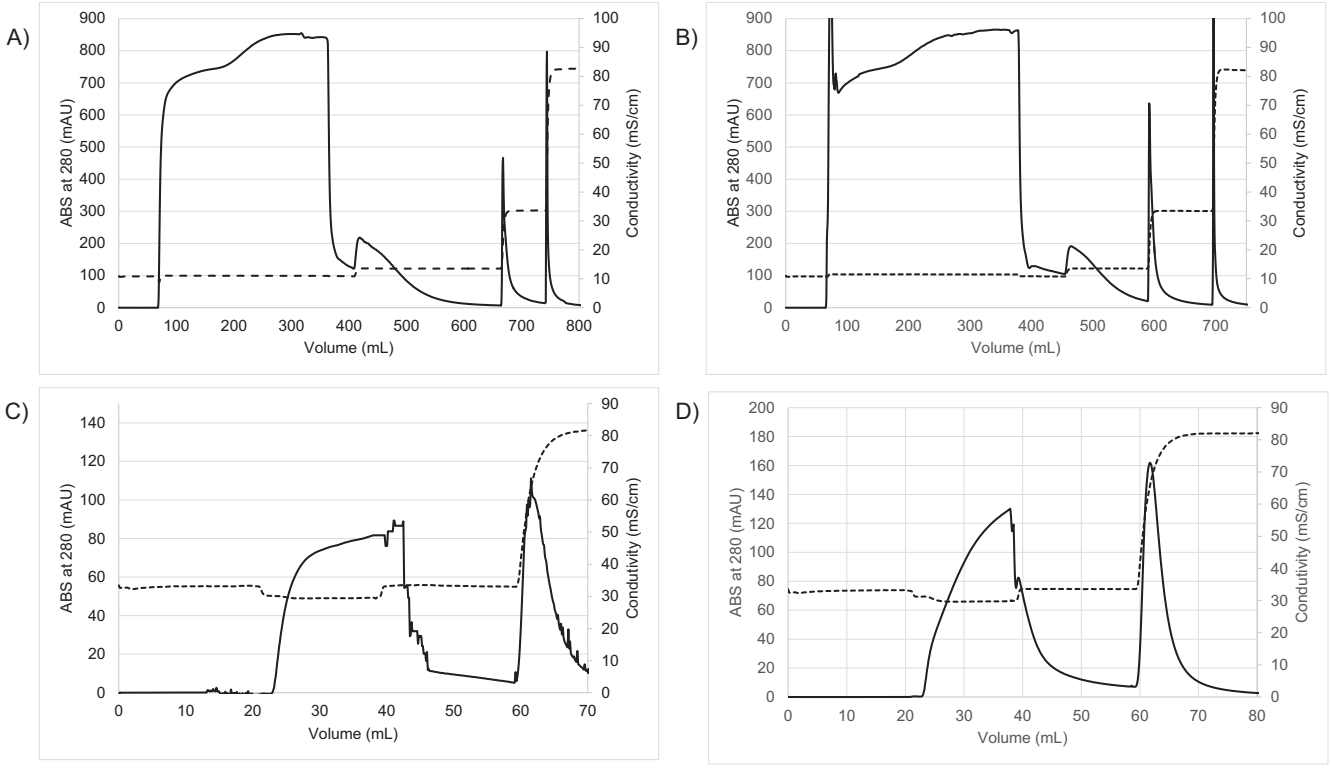

Fig. 3. Complete two-step purification process. (A) chromatogram of the capture step (Q anion-exchange chromatography) for zika VLPs. (B) chromatogram of the capture step for YF VLPs. (C) chromatogram of the second purification step (multimodal CaptoCore 700 resin) for zika VLPs. (D) chromatogram of the second purification step for YF VLPs. For all graphs, solid lines represent the absorbance at 280 nm and dashed lines represent the conductivity.

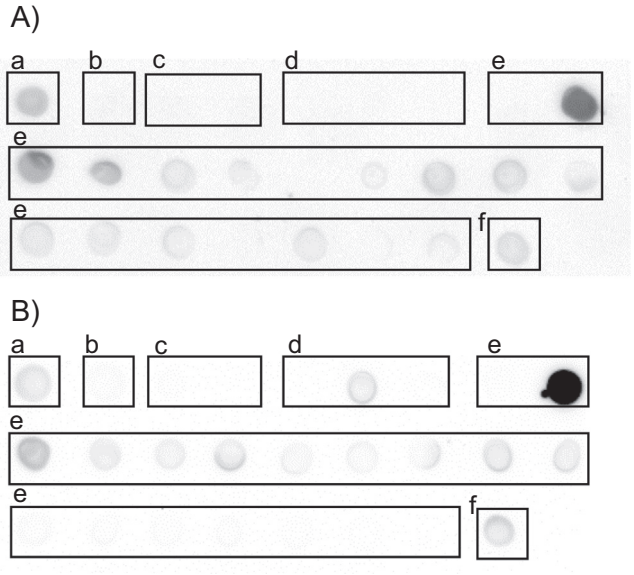

Fig. 4. Immunoblot of the fractions from the anion-exchange chromatography step shown in Fig. 3A and B, for zika (A) and yellow fever (B). In both panels the fractions are: (a) clarified supernatant; (b) flow-through collected during loading; (c) wash at 9% buffer B collected in two fractions containing 10 mL; (d) wash at 12% buffer B collected in three fractions containing 3 mL; (e) elution at 35% buffer B in eighteen fractions containing 3 mL; (f) wash at 100% buffer B.

zika and YF VLP preparations (151–178 μg/mL) was in the same order of magnitude as the VLP concentration measured by ELISA (169–175 μg/mL). Although a direct comparison is not possible due to the different principles of the quantification methods, the order-of-magnitude matching indicates an efficient removal of protein impurities and a high purity level of the samples.

Regarding the purified YF VLPs, supposing the same dose size as Pato et al. [26] considered for an inactivated yellow fever vaccine candidate (8 μg measured in the virus preparations by E-protein ELISA), the purification process described herein resulted in a DNA level in the purified YF VLP preparation of 1.37 ng/dose. Considering the limit of 10 ng/dose established by regulatory authorities [16,25,36], this limit would just be reached in our YF VLP preparation for a dose size of 58 μg.

In the case of zika VLPs, Espinosa et al. [37] tested in mice doses of 1 to 25 μg of zika VLPs produced in transiently transfected HEK293 cells, adjuvanted or not with alum. When alum was used, a strong dose-sparing effect was observed and the titers of neutralizing antibodies (nAb) were increased by 5 (after prime immunization) to 7 fold (after boost immunization). For the adjuvanted VLP preparation, the lowest dose tested (1 μg) generated nAb titers as high as the titers obtained for the highest (25 μg) non-adjuvanted VLP preparation. These nAb titers of the 1-μg adjuvanted VLP preparation were high enough to protect against challenge immunosuppressed mice receiving passive transfer of immune serum [37]. Considering our purified zika VLPs, the 10 ng DNA per dose regulatory limit would be reached for a dose size of 28 μg, thus providing enough room to increase dose size for human use. Therefore, the DNA clearance given by the downstream process proposed herein seems to ensure that host-cell DNA meets regulatory requirements after the two steps of chromatography.

3.3. VLP characterization

The presence of the flavivirus envelope protein was confirmed with the expected molecular mass (50–55 kDa) [38] by Western blotting for both zika (Fig. 5A) and yellow fever VLPs (Fig. 5B), and a dimeric form of the envelope protein at approximately

Table 1
Overview of performance of the two-step chromatography purification process.

VLP type	Step	Volume (mL)	[VLP] (μg/mL)	VLP mass (μg)	[Total protein] (μg/mL)	Total protein (μg)	VLP-to-TP (mg_{VLP}/mg_{TP})	Total protein removal (%)	Yield (%)	Purification factor (-)	[DNA] (μg/mL)	DNA (μg)	DNA removal (-)
Zika VLPs	Supernatant	290	15.8	4582.0	–	–	–	–	–	–	–	–	–
	Clarified supernatant	290	13.3	3857.0	207.3	60117.0	0.06	–	84.2	–	2.18	632.20	–
	Q Eluate	18	185.8	3344.4	299.2	5385.6	0.62	91.0	86.7	9.7	1.04	18.72	97.0
	CC700 flow-through	18	168.9	3040.2	151.4	2725.2	1.12	49.4	90.9	1.8	0.06	1.08	94.2
	Overall	–	–	–	–			95.5	66.4	17.4	–	–	99.8
Yellow fever VLPs	Supernatant	315	14.7	4630.5	–	–	–	–	–	–	–	–	–
	Clarified supernatant	315	11.7	3685.5	118.3	37264.5	0.10	–	79.6	–	2.28	718.20	–
	Q Eluate	18	195.5	3519.0	365.2	6573.6	0.54	82.4	95.5	5.4	0.92	16.56	97.7
	CC700 flow-through	18	175.3	3155.4	178.0	3204.0	0.98	51.3	89.7	1.8	0.03	0.54	96.7
	Overall	–	–	–	–			91.4	68.1	10.0	–	–	99.9

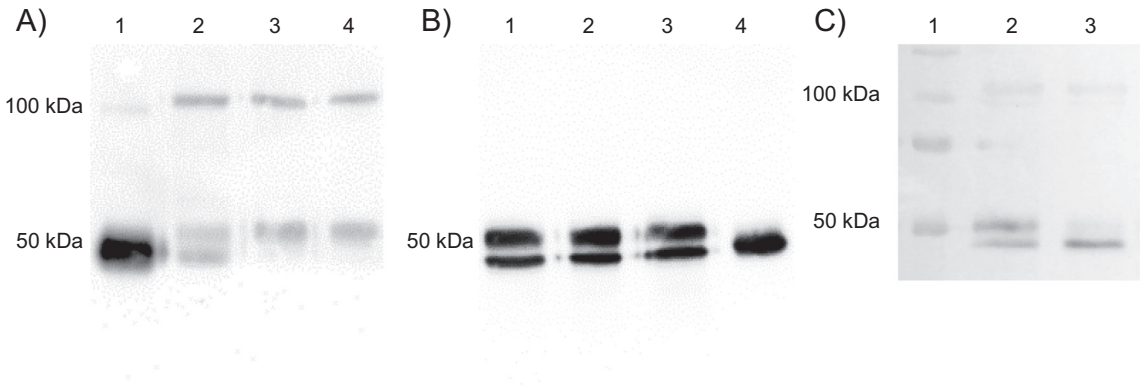

Fig. 5. (A) Western blot of samples of zika VLPs from each purification step: Dengue virus serotype 2 envelope protein standard (Denv2-ENV-100, Native Antigen Company, UK), 15 μL of 30 μg/mL solution (lane 1); cell culture supernatant (lane 2); elution peak from anion exchange (AEX) step (lane 3); flow-through from multimodal step (lane 4). (B) Western blot of samples of yellow fever VLPs from each purification step: cell culture supernatant (lane 1); elution peak from AEX step (lane 2); flow-through from multimodal step (lane 3); Dengue E standard (Denv2-ENV-100), 15 μL of 30 μg/mL solution (lane 4). (C) Western blot of purified YF VLPs for investigation of the presence of glycosylated variants: molecular mass marker (lane 1); flow-through from multimodal chromatography step (lane 2); flow-through from multimodal chromatography step after PNGase F digestion (lane 3).

100 kDa could additionally be observed in the case of zika VLPs. This E dimer is equally observed in the certificate of analysis of zika VLPs commercialized by a world leading supplier of infectious disease antigens [39]. Moreover, since two discrete bands were observed around 50–55 kDa in the Western blots, a digestion of the YF VLPs with PNGase F was performed to evaluate if the two bands were related to different glycosylation patterns of the E protein. As shown in Fig. 5C, after PNGase F digestion the band with higher molecular mass disappeared, and the lower band became stronger, giving evidence of the presence of a mixture of glycosylated and non-glycosylated forms of the E protein. Espinosa et al. [37] observed by SDS-PAGE and Western blotting that recombinant E protein produced by transiently transfected HEK293 cells and insect cells differed in molecular mass, and postulated that this difference was due to the more simple glycosylation pattern in the recombinant protein produced by insect cells.

Transmission electron microscopy (negative staining TEM) was carried out to observe the VLPs after purification. Fig. 6A shows purified zika VLPs, whereas purified YF VLPs are shown in Fig. 6B. Tridimensional structures approximately 50 nm in size were observed, similarly as verified by Pato et al. [26] for the whole YF virus, confirming the successful production and purification of these flavivirus VLPs.

In order to confirm the size of VLPs, further analyses were carried out by dynamic light scattering (DLS). For zika VLPs it was possible to do the DLS analysis shortly (2 days) after VLP purification (Fig. 7A). The narrow size distribution indicated an average zika VLP diameter of 45.2 nm. This is in agreement with Espinosa et al. [37], who produced zika VLPs by transient transfection of HEK293 cells and found by TEM that most particles had diameters in the range of 35 to 55 nm.

For YF VLPs, due to limitations regarding the use of the equipment, the DLS analysis could be carried out only three weeks after VLP purification, so that the YF VLPs were kept in the purification buffer (PBS buffer containing 350 mM NaCl) at 4 °C for this time interval. The DLS data shown in Fig. 7B shows that YF VLPs had a diameter of approximately 54.4 nm, but that aggregates in the range of 200–400 nm, probably tetramers to octamers of YF VLPs, were present. Aggregation over time when VLPs are stored in salt-containing solutions is a commonly reported issue [40,41], which is confirmed by Fig. 7A (fresh zika VLP samples) and 7B (YF VLP samples stored for a longer period in PBS + 350 mM NaCl). Thus, the present DLS data confirm that our purified VLPs had the size expected for flaviviruses, but indicate that buffer exchange shortly after VLP purification is highly recommended in order to avoid aggregation.

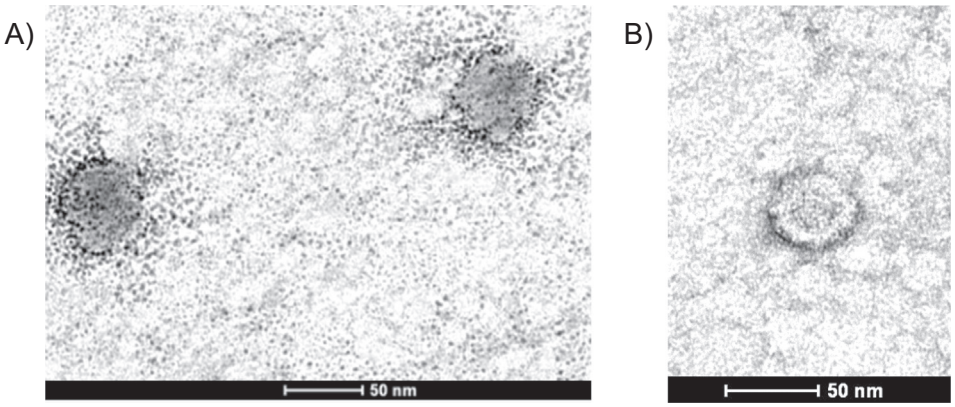

Fig. 6. Transmission electron micrographs of purified samples. (A) zika VLPs. (B) YF VLPs.

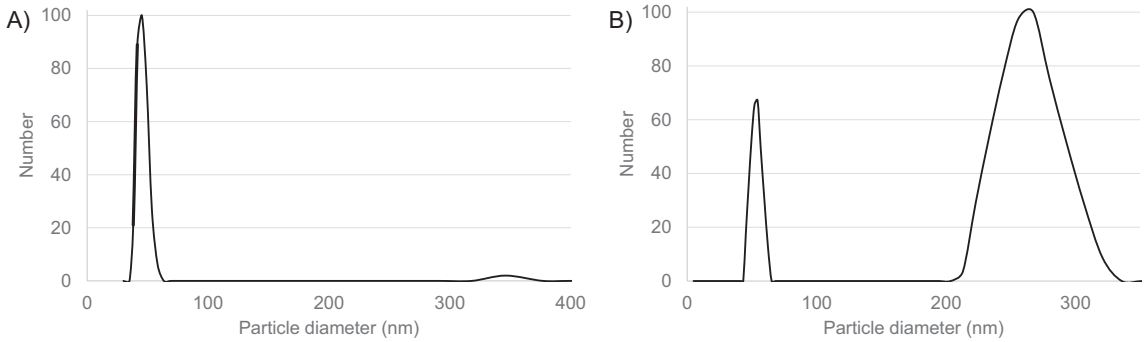

Fig. 7. Size distribution of particles in purified VLP samples measured by DLS. (A) zika VLPs after 2 days of storage at 4 °C. (B) yellow fever VLPs after 3 weeks of storage at 4 °C.

4. Conclusions

In the present work a 2-step chromatography process was evaluated for the purification of zika and yellow fever virus-like particles produced by stably transfected HEK293-3F6 cells. A capture step based on a strong anion-exchange membrane adsorber allowed processing of clarified cell culture supernatants at high flow rates, enabled a significant decrease (82–91%) in total protein amount and promoted an approximately 15-fold concentration of VLPs, with 97–98% removal of host-cell DNA, at VLP yields ranging from 86.7% for zika VLPs to 95.5% for YF VLPs. The second chromatography step, based on a multimodal chromatography resin, promoted a further decrease in total protein and host-cell DNA, at VLP yields of approximately 90% for both VLPs. Overall, the global VLP purification yield, including the clarification step, was 66.4% for zika VLPs and 68.1% for YF VLPs, which is promising for large-scale implementation. DNA clearance potential of the purification process was demonstrated, since 99.8 to 99.9% DNA removal was achieved, yielding DNA levels lower than the limits established by the World Health Organization. Characterization of the purified VLPs by dynamic light scattering (DLS) and transmission electron microscopy showed that both structure and size of zika and YF VLPs were as expected for flaviviruses. DLS data further indicated that a buffer exchange or excipient addition is needed to avoid VLP aggregation along storage time.

The promising results obtained for the purification of zika and yellow fever VLPs indicate that this process could also potentially be applied to other flavivirus VLPs that we have expressed in our lab, such as DENV1-4, Saint Louis encephalitis virus, West Nile virus, Cacipacore virus and Ilheus virus. Overall, the downstream process presented herein, coupled to the stable, constitutive VLP expression platform and to the production by continuous perfusion bioreactor cultures established in our lab [30], could potentially represent a simple, robust and economic technology for the production of cell culture-derived recombinant flavivirus vaccines.

Funding

Financial support from the Brazilian research funding agencies CNPq, Capes and Faperj is gratefully acknowledged.

Declaration of Competing Interest

The authors declare no conflict of interest.

Acknowledgements

T. P. Pato (Biomanguinhos/FIOCRUZ, Brazil) for fruitful discussions; B. S. Graham (VRC, NIH, USA) for sharing reagents; L. Caldas (CENABIO/UFRJ, Brazil) for carrying out the TEM analyses; LATAM Laboratory (Biomanguinhos/FIOCRUZ, Brazil) for providing the 4G2 monoclonal antibody; S. F Carvajal (Hertha Meyer Ultrastructure and Cellular Biology Laboratory, UFRJ, Brazil) for the use of the DLS equipment and fruitful discussions; W. S. Abreu (COPPE/UFRJ, Brazil) for help with the PNGase F study; and R. G. F. Alvim (COPPE/UFRJ, Brazil) for supplying the cell culture supernatants containing the VLPs.

All authors attest they meet the ICMJE criteria for authorship.

References

[1] Mukhopadhyay S, Kuhn JR, Rossmann MG. A structural perspective of the flavivirus life cycle. Nat Rev Microbiol 2005;3(1):13–22.
[2] Kaaijk P, Luytjes W. Are we prepared for emerging flaviviruses in Europe? Challenges for vaccination. Hum Vacc Immunotherap 2017;14(2):337–44.
[3] Klitting R, Gould EA, Paupy C, Lamballerie X. What does the future hold for yellow fever virus? Genes 2018;9:E291.
[4] Changa C, Ortiz K, Ansari A, Gershwin ME. The Zika outbreak of the 21st century. J Autoimmun 2016;68:1–13.
[5] Roth A, Mercier A, Lepers C, Hoy D, Duituturaga S, Benyon E, et al. Concurrent outbreaks of dengue, chikungunya and Zika virus infections – an unprecedented epidemic wave of mosquito-borne viruses in the Pacific 2012–2014. Euro Surveillance 2014;19(41).
[6] PAHO/WHO. Zika cases and congenital syndrome associated with Zika virus reported by countries and territories in the Americas, 2015–2018 Cumulative cases. <https://www.paho.org/hq/index.php?option=com_docman&view=download&category_slug=cumulative-cases-pdf-8865&alias=43296-zika-cumulative-cases-4-january-2018-296&Itemid=270&lang=en> [accessed November 06, 2018].
[7] Brasil P, Pereira JP, Moreira ME, Nogueira RMR, Damasceno L, Wakimoto M, et al. Zika virus infection in pregnant women in Rio de Janeiro. N Engl J Med 2016;375:2321–34.
[8] Barzon L, Palù G. Current views on Zika virus vaccine development. Expert Opin Biol Ther 2017;17(10):1185–92.
[9] Song BH, Yun SI, Woolley M, Lee YM. Zika virus: History, epidemiology, transmission, and clinical presentation. J Neuroimmunol 2017;308:50–64.
[10] Gardner CL, Ryman KD. Yellow fever: a reemerging threat. Clin Lab Med 2010;30(1):237–60.
[11] Paules CI, Fauci AS. Yellow fever - once again on the radar screen in the Americas. N Engl J Med 2017;376(15):1397–9.
[12] Foster KR, Jenkins MF, Toogood AC. The Philadelphia Yellow Fever Epidemic of 1793. Sci Am 1998;279:88–93.
[13] Soler JC, Fusté MRP, Herràndiz RA, Adell CN, Lawrence RS. A mortality study of the last outbreak of yellow fever in Barcelona City (Spain) in 1870. Gac Sanit 2009;23(4):295–9.
[14] Goldani LZ. Yellow fever outbreak in Brazil, 2017. Braz J Infect Dis 2017;21(2):123–4.
[15] Shearer FM, Moyes CL, Pigott DM, Brady OJ, Marinho F, Deshpande A, et al. Global yellow fever vaccination coverage from 1970 to 2016: an adjusted retrospective analysis. Lancet Infect Dis 2017;17(11):1209–17.
[16] WHO. WHO position on the use of fractional doses - June 2017, addendum to vaccines and vaccination against yellow fever WHO: Position paper - June 2013. Vaccine 2017; 35(43):5751–2.
[17] Litvoc MN, Novaes CTG, Lopes MIBF. Yellow fever. Revista da Associação Médica Brasileira 2018;64(2):106–13.
[18] de Menezes Martins R, Maia MLS, de Lima SMB, de Noronha TG, Xavier JR, Camacho LAB. Duration of post-vaccination immunity to yellow fever in volunteers eight years after a dose-response study. Vaccine 2018;36(28):4112–7.

[19] Wasserman S, Tambyah PA, Lim PL. Yellow fever cases in Asia: primed for an epidemic. Int J Infect Dis 2016;48:98–103.
[20] Grgacic EV, Anderson DA. Virus-like particles: passport to immune recognition. Methods 2006;40(1):60–5.
[21] Roldão A, Mellado MC, Castilho LR, Carrondo MJ, Alves PM. Virus-like particles in vaccine development. Expert Rev Vacc 2010;9(10):1149–76.
[22] Dai S, Wang H, Deng F. Advances and challenges in enveloped virus-like particle (VLP)-based vaccines. J Immunol Sci 2018;2(2):36–41.
[23] Vicente T, Roldão A, Peixoto C, Carrondo MJ, Alves PM. Large-scale production and purification of VLP-based vaccines. J Invertebr Pathol 2011;107: S42–8.
[24] Ohtaki N, Takahashi H, Kaneko K, Gomi Y, Ishikawa T, Higashi Y, et al. Purification and concentration of non-infectious West Nile virus-like particles and infectious virions using a pseudo-affinity Cellufine Sulfate column. J Virol Methods 2011;174:131–5.
[25] Pato TP, Souza MC, Silva AN, Pereira RC, Silva MV, Caride E, et al. Development of a membrane adsorber based capture step for the purification of yellow fever virus. Vaccine 2014;32(24):2789–93.
[26] Pato TP, Souza MC, Mattos DA, Caride E, Gaspar LP, Freire MS, et al. Purification of yellow fever virus produced in Vero cells for inactivated vaccine manufacture. Vaccine 2019;37:3214–20.
[27] Vicente T, Sousa MFQ, Peixoto C, Mota JPB, Alves PM, Carrondo MJT. Anion-exchange membrane chromatography for purification of rotavirus-like particles. J Membr Sci 2008;311:270–83.
[28] Vogel JH, Nguyen H, Giovannini R, Ignowski J, Garger S, Salgotra A, et al. A new large-scale manufacturing platform for complex biopharmaceuticals. Biotechnol Bioeng 2012;109(12):3049–58.
[29] Middelberg PJA, Lua LHL. Virus-like particle bioprocessing: challenges and opportunities. Pharmaceut Bioprocess 2013;1(5):407–9.
[30] Alvim RG, Itabaiana Jr I, Castilho LR. Zika virus-like particles (VLPs): stable cell lines and continuous perfusion processes as a new potential vaccine manufacturing platform. Vaccine 2019;37(47):6970–7. https://doi.org/10.1016/j.vaccine.2019.05.064.
[31] Ellis KJ, Morrison JF. Buffers of constant ionic strength for studying pH-dependent processes. Methods Enzymol 1982;87:405–26.
[32] Hughson M, Cruz T, Carvalho R, Castilho L. Development of a 3-step straight-through purification strategy combining membrane adsorbers and resins. Biotechnol Prog 2017;33(4):931–40.
[33] Ladd Effio C, Hahn T, Seiler J, Oelmeier S, Asen I, Silberer C, Villain L, Hubbuch J. Modeling and simulation of anion-exchange membrane chromatography for purification of Sf9 insect cell-derived virus-like particles. J Chromatogr A 2016;1429:142–54.
[34] Nestola P, Peixoto C, Villain L, Alves PM, Carrondo MJT, Mota JPB. Rational development of two flowthrough purification strategies for adenovirus type 5 and retro virus-like particles. J Chromatogr A 2015;1426:91–101.
[35] Zhao D, Sun B, Jiang H, Sun S, Kong F, Ma Y, et al. Enterovirus71 virus-like particles produced from insect cells and purified by multistep chromatography elicit strong humoral immune responses in mice. J Appl Microbiol 2015;119 (4):1196–205.
[36] World Health Organization. WHO Study Group on cell substrates for production of biologicals. Geneva: WHO Headquarters; 2007.
[37] Espinosa D, Mendy J, Manayani D, Vang L, Wang C, Richard T, et al. Passive transfer of immune sera induced by a Zika virus-like particle vaccine protects AG129 mice against lethal Zika virus challenge. EBioMedicine 2018;27:61–70.
[38] Native Antigen Company (NAC). Dengue virus serotype 2 envelope protein (HEK293); 2019. <https://thenativeantigencompany.com/products/dengue-virus-serotype-2-envelope-protein/> [accessed April 30, 2019].
[39] Native Antigen Company (NAC). Zika Virus VLP – Certificate of Analysis; 2019. <https://thenativeantigencompany.com/wp-content/uploads/2018/10/CofA-ZIKV-VLP-100-Batch17061910-new-address.pdf> [accessed April 30, 2019].
[40] Shi L, Sanyal G, Ni A, Luo Z, Doshna S, Wang B, et al. Stabilization of human papillomavirus virus-like particles by non-ionic surfactants. J Pharm Sci 2005;94(7):1538–51.
[41] Chen Y, Zhang Y, Quan C, Luo J, Yang Y, Yu M, Kong Y, Ma G, Su Z. Aggregation and antigenicity of virus like particle in salt solution - A case study with hepatitis B surface antigen. Vaccine 2015;33(35):4300–6.